Research in Astron. Astrophys. **2013** Vol. **13** No. **4**, 373–386
http://www.raa-journal.org *http://www.iop.org/journals/raa*

Research in Astronomy and Astrophysics

Semi-numerical simulation of reionization with semi-analytical modeling of galaxy formation *

Jie Zhou[1], Qi Guo[1], Gao-Chao Liu[1,2], Bin Yue[1], Yi-Dong Xu[1] and Xue-Lei Chen[1,3]

[1] National Astronomical Observatories, Chinese Academy of Sciences, Beijing 100012, China; *xuelei@cosmology.bao.ac.cn*
[2] College of Science, China Three Gorges University, Yichang 443002, China
[3] Center of High Energy Physics, Peking University, Beijing 100871, China

Received 2012 October 26; accepted 2012 October 31

Abstract In a semi-numerical model of reionization, the evolution of ionization fraction is approximately simulated by the criterion of ionizing photon to baryon ratio. We incorporate a semi-analytical model of galaxy formation based on the Millennium II N-body simulation into the semi-numerical modeling of reionization. The semi-analytical model is used to predict the production of ionizing photons, then we use the semi-numerical method to model the reionization process. Such an approach allows more detailed modeling of the reionization, and also connects observations of galaxies at low and high redshifts to the reionization history. The galaxy formation model we use was designed to match the low-z observations, and it also fits the high redshift luminosity function reasonably well, but its prediction about star formation falls below the observed value, and we find that it also underpredicts the stellar ionizing photon production rate, hence the reionization cannot be completed at $z \sim 6$. We also consider simple modifications of the model with more top heavy initial mass functions, which can allow the reionization to occur at earlier epochs. The incorporation of the semi-analytical model may also affect the topology of the HI regions during the epoch of reionization, and the neutral regions produced by our simulations with the semi-analytical model, which appeared less poriferous than the simple halo-based models.

Key words: cosmology: reionization — galaxies: formation

1 INTRODUCTION

The reionization of hydrogen gas in the universe has been a topic of forefront research in recent years. The measurement of the cosmic microwave background (CMB) polarization by the Wilkinson Microwave Anisotropy Probe (WMAP) indicates that the reionization occurred at $z_{\rm reion} = 10.6 \pm 1.2$, assuming an instant reionization model (Larson et al. 2011). We also anticipate more precise measurements from the Planck satellite (Mitra et al. 2011; Ahn et al. 2012). On the other hand, observations of high redshift quasars show the presence of a Gunn-Peterson trough at $z \sim 6$, which marked the end of the hydrogen reionization process (Becker et al. 2001; Fan et al. 2002). While

* Supported by the National Natural Science Foundation of China.

we still do not have detailed knowledge about the nature of the ionizing photon sources, Rauch et al. (1997) found that for the observed luminosity function, high redshift quasars failed to produce enough ionizing photons to keep the universe ionized before $z \sim 4$, thus the stars probably contributed the majority of ionizing photons, but the fractions of different stellar populations and the quasars are presently unknown. However, as the capability of space and ground based optical/infrared telescopes has improved, we are learning more and more about the galaxies at the epoch of reionization (EoR) (Ota et al. 2010; Wilkins et al. 2010; Bunker et al. 2010; Lorenzoni et al. 2011; Yan et al. 2011a,b; Bouwens et al. 2012; Bradley et al. 2012). Moreover, hundreds of gamma-ray bursts (GRBs) have been detected by the SWIFT and Fermi spacecraft (Salvaterra 2012); many of these are at high redshifts, with the highest ones, e.g. GRB 090429B and GRB 090423 at $z > 8$, and they provide additional information on the star formation history during the EoR (Ishida et al. 2011).

The 21cm emission from the high redshift intergalactic medium (IGM) could potentially allow us to directly observe the EoR, providing three-dimensional information about the evolution and morphology of the reionization process (Madau et al. 1997). However, it is difficult to detect this signal with the presence of strong foregrounds. Attempts have been made with the EDGES experiment (Bowman & Rogers 2010), and GMRT EoR search (Paciga et al. 2011; Pen et al. 2009). Several low frequency radio telescope arrays have been or are being built to detect this signal, including the 21CMA[1], the Mileura Wide Field Array (MWA) (Joudaki et al. 2011), the Low Frequency Array (LOFAR) (Harker et al. 2010), and PAPER (Parsons et al. 2010). In the future, HERA (Furlanetto et al. 2009) and the Square Kilometer Array (SKA) (Santos et al. 2011) may provide even more powerful observational probes.

Detailed modeling of reionization is required to interpret various observational data. An accurate numerical model must include treatment of gas dynamics, chemistry, feedback processes, and especially, radiative transfer of ionizing photons. Many groups have conducted radiative transfer simulations to study the EoR (Gnedin 2000; Razoumov et al. 2002; Ciardi et al. 2003; Sokasian et al. 2001; Maselli et al. 2003; Mellema et al. 2006; McQuinn et al. 2007; Trac & Cen 2007; Altay et al. 2008; Aubert & Teyssier 2008; Finlator et al. 2009; Petkova & Springel 2009). However, such simulations have extremely high demands on computing resources. High resolution is required to resolve low mass galaxies, which may contribute a significant fraction of ionizing photons, but as the typical size of the ionized regions at the end of EoR is expected to be tens of comoving Mpc, a large simulation box is also required to statistically sample the distribution of HII regions. This large dynamic range puts severe demands on the computational cost of the simulation. Furthermore, since our knowledge about high redshift galaxies is still very rudimentary, we need to explore a large range of parameter space, but the high computational cost makes this difficult or impossible to do. For these reasons, it is worthwhile to make simpler but faster models to gain some physical insights and explore the parameter space.

Inspired by the results of numerical simulations with radiative transfer computation of ionizing photons, an analytical model known as the "bubble model" was developed (Zaldarriaga et al. 2004; Furlanetto et al. 2004b,a). It uses an excursion set formulation of structure formation to study the size distribution of ionized regions and the induced 21cm emission power spectrum. In this model, whether a region is ionized or not is determined by the ratio of the number of ionizing photons produced locally and in the surrounding regions to the number of baryons. This model is intuitive, and allows one to analytically calculate the size distribution of the HII regions during the EoR. This method is then extended to the so called semi-numerical model (Zahn et al. 2007; Mesinger & Furlanetto 2007; Zahn et al. 2011; Mesinger et al. 2011). First order perturbation theory is used to produce the halo distribution function at any given redshift, then the star formation rate (SFR) and the number of ionizing photons produced is calculated. Finally, the same ionizing photon-to-baryon ratio criterion is used to obtain the ionization field from the halo field. Zahn et al. (2011)

[1] *http://trend.bao.ac.cn/index.html*

compared this algorithm with a ray-tracing radiative transfer simulation, and found that they are in good agreement, even though it only costs a tiny fraction of the computing time compared to the full radiative transfer simulation. However, these semi-numerical models do not consider the galaxy formation process in detail.

The galaxy formation process is complicated. Besides the nonlinear evolution of dark matter density fluctuations, it involves the heating and cooling of gas, ionization and recombination, formation of molecules and chemical enrichment, formation of stars and the feedback process. Limited by the dynamic range of simulations and our knowledge about the complex physics of these processes, all numerical simulations have to adopt some kind of phenomenological approximation. In the so called semi-analytical modeling approach, galaxy formation processes, especially star formation, are simulated by following a set of prescriptions based on the property of the dark matter halos, and after specifying some model parameters, it can be used to predict the observational properties of galaxies, such as luminosity function, stellar age and metal distribution at different redshifts. The model parameters are adjusted to fit the observations. Compared with hydrodynamic simulations, the major advantage of the semi-analytical model is that it has much lower computational cost, so a large range of parameter space can be explored without repeating the whole simulation. Semi-analytical modeling has become a powerful tool of cosmological investigation, and over the years the models have been developed to incorporate more physical details, and to provide predictions of more observations (White & Frenk 1991; Kauffmann et al. 1993; Cole et al. 1994; Kauffmann et al. 1999; Somerville & Primack 1999; Cole et al. 2000; Springel et al. 2001; Hatton et al. 2003; Croton et al. 2006; Bower et al. 2006; De Lucia & Blaizot 2007; Guo & White 2009; Weinmann et al. 2010).

Recent semi-analytical models can fit the observational data such as the luminosity and mass distributions of galaxies and quasars, the history of star formation and quasar evolution, and also the correlation of a number of observable properties of galaxies and quasars (Bower et al. 2006; De Lucia & Blaizot 2007). Semi-analytical modeling has also been used to study the high redshift universe, for example, Raičević et al. (2011) used the Durham GALFORM model to investigate the reionization history. They compared the number of ionizing photons with the number of hydrogen atoms in different models of initial stellar mass functions, and found that the stellar components were enough to ionize the universe at $z \sim 10$.

In the present paper, we introduce the semi-analytical modeling of galaxy formation into the semi-numerical model of reionization. The semi-analytical model provides more detailed information about galaxy formation and the production of ionizing photons. More importantly, this allows us to compare the EoR models and probe the observations at lower redshifts, so that eventually a self-consistent model of galaxy formation and reionization could be developed. We use the semi-analytical model developed by Guo et al. (2011), which is based on the Millennium (MS) and Millennium II (MS II) N-body simulations (Boylan-Kolchin et al. 2009). By modeling a number of physical processes in a plausible way, and after tuning the parameters, this model successfully reproduced many observables, such as the luminosity function and SFR. We then use the density field from the same MS II, with the baryon density tracing the dark matter density, and the semi-numerical model of Zahn et al. (2011) to calculate the evolution of ionization fraction.

This paper is organized as follows. In Section 2 we briefly review the semi-numerical algorithm, and in Section 3 we introduce the semi-analytic model and describe our improvements. In Section 4 we show our result of the reionization history and morphology. In Section 5 we discuss our parameter space and summarize our results.

2 SEMI-NUMERICAL SIMULATION

The semi-numerical model of reionization (Zahn et al. 2011; Mesinger et al. 2011) is an extension of the analytical bubble model (Furlanetto et al. 2004b). It is assumed that before the completion of the reionization process of the IGM, a number of HII regions will appear in the IGM, and they

are preferentially located in regions of higher densities, because in such regions structures formed earlier. The mass of each HII region is proportional to the number of ionizing photons produced within the region, and the criterion for ionization of the region is $f_{\rm coll} > \xi^{(-1)}$, where ξ is the efficiency parameter. It could be written as $\xi = f_{\rm esc} f_* N_\gamma / N_{\rm rec}$, where $f_{\rm esc}$ is the fraction of ionizing photons which escaped the halo into the IGM, f_* is the fraction of baryons in stars in the halo, N_γ is the number of photons emitted per baryon in the stars, and $N_{\rm rec}$ is the average number of recombinations. We can rewrite the reionization criterion as

$$\delta_m > \delta_x(m, z) \tag{1}$$

where

$$\delta_x(m, z) = \delta_c - \sqrt{2} K(\xi) [\sigma^2_{\rm min} - \sigma^2(m)]^{-1/2} \tag{2}$$

and $K(\xi) = {\rm erf}^{-1}(1 - \xi)$. A point in a region of mass m is marked as ionized if and only if the scale m is the largest scale for which the condition Equation (1) is satisfied. The mass function of the HII regions can then be obtained. For normal stars, it was estimated that a plausible set of parameters is $f_* \sim 0.2$, $N_\gamma \sim 3200$, $f_{\rm esc} \sim 0.05$, and $N_{\rm rec} \sim 3$, so $\xi \sim 10$. However, there are large uncertainties in all of these parameter values. For example, most low redshift observations indicate $f_{\rm esc} < 5\%$, but the escape fraction at high redshifts might be much larger. Observations of galaxies at $z = 1 - 3$ indicate a broad range of escape fraction values from a few percent to tens of percent (Shapley et al. 2006; Siana et al. 2007; Grazian et al. 2011; Iwata et al. 2009). ξ is also very uncertain, and at present vastly different choices of ξ value are possible (Furlanetto et al. 2004b).

Zahn et al. (2011) and Mesinger et al. (2011) generalized the analytical bubble model to what they called semi-numerical simulations, and the latter, known as the `21cmFAST`, are publicly available. The procedure for performing such calculations is:

(1) create the linear density and velocity fields;
(2) find halos from the density field;
(3) reallocate the halo position by first order perturbation theory;
(4) generate the ionizing field by the equation: $\xi * m_{\rm gal} > m_{\rm H}$.

In steps 2 and 4, the formation criterion is checked from large scales down to each single cell of the simulation box to flag a halo or an HII region. Once the criterion is satisfied, a halo is generated (in step 2) or an ionized region is marked. For the ionization, one could either flag all pixels inside the region as ionized, or only flag the center pixel as ionized. Obviously, the latter is much faster, but the results turned out to show no significant difference. Zahn et al. (2011) compared their result with a radiative transfer simulation with the same initial conditions, and found the result of the semi-numerical simulation was a good approximation of the radiative transfer simulation. Thus, the semi-numerical algorithm captures the bubble topology and reionization history quite well with a moderate amount of computation.

In this paper, we further improve the semi-numerical model by implementing a more detailed model of ionizing photon production based on the semi-analytic model of galaxy formation. Both the semi-numerical model of reionization and the semi-analytical model of galaxy formation are efficient in terms of computation, so our model still allows relatively quick exploration of the parameter space. Moreover, this approach also allows us to investigate how the physical processes affect the reionization history, and to constrain the reionization model parameters with galaxy observations.

To include the physical process in the galaxies, we rewrite the ionizing criterion as

$$\frac{N_\gamma f_{\rm esc}}{N_{\rm rec}} > N_{\rm IGM}, \tag{3}$$

where $N_{\rm IGM}$ is the hydrogen number density in the IGM. The MS II is a pure dark matter simulation, and we assume that the baryon density traces the dark matter density, $\rho_{\rm b} = \rho_{\rm d} * \Omega_{\rm b} / \Omega_m$. For the

reionization simulation, we smooth the density field on to a 256^3 grid. We calculate N_γ for each galaxy by relating its UV luminosity to the SFR, and by integrating this luminosity through its formation history we could get the total number of ionizing photons. Our algorithm is:

(1) convert the dark matter density field in the MS II to the IGM density field;
(2) locate galaxies from the semi-analytical model in the simulation box and calculate the ionizing photon number;
(3) generate the ionizing field by Equation (3).

In step 2, we assume that for ordinary Pop I stars the total number of ionizing photons is similar to the value given in Furlanetto et al. (2004b). However, we also test how the stellar population affects the ionizing history. In our *model C* (see next section) we treat the luminosity as a function of metallicity. In step 3, using the same method as Zahn et al. (2011), we check for each pixel whether the ionizing criterion is satisfied at a large scale comparable with the simulation box; once the criterion is satisfied, we flag all pixels inside the region as ionized, or if not, we move into a smaller radius to repeat the above process, till the region is ionized or we have reached a single pixel.

The effect of recombination at high redshift is quite complicated, and, since the purpose of this paper is to develop a relatively fast method to study the ionizing history and the morphology of HII regions, here we shall make a simple assumption of a constant number of recombinations (see Yue & Chen 2012 for an example of sophisticated modeling of the evolution of recombination rate). Here we adopt $N_{\rm rec} = 3$.

3 SEMI-ANALYTICAL MODEL

In the hierarchical structure formation scenario, the dark matter halos grow by accretion and merger, and galaxies form within dark matter halos by the radiative cooling of the baryonic gas. In semi-analytical models, one follows the evolution of each dark matter halo, and applies a set of rules to describe the gas cooling, star formation and feedback for each halo without actual simulations. The properties of the galaxies within each halo, such as the stellar mass, the age of the stellar population, the distribution within halos, the amount of cold and hot gas, and metal abundance, can be followed. The dark matter halo merger tree is generated either by Monte-Carlo simulations (White & Frenk 1991; Kauffmann et al. 1993; Cole et al. 1994), or by using an N-body simulation. With improvement in computing power, in most recent works the latter approach is adopted (Bower et al. 2006; Croton et al. 2006; De Lucia & Blaizot 2007; Guo & White 2009; Weinmann et al. 2010).

For galaxy formation modeling during the EoR, high resolution simulations are required. Indeed, it is believed that the first stars form in halos of $10^6\ M_\odot$, and the first galaxies have masses about $10^8\ M_\odot$ (c.f. Barkana & Loeb 2001). At the same time, the model should also contain enough volume such that a large number of neutral or ionized regions can be included in the simulation at the EoR. In this work, we use a model based on the MS II (Boylan-Kolchin et al. 2009). This is an extension of the earlier MS (Springel et al. 2005), and is among the largest cosmological N-body simulations with sufficient mass resolution that is currently available. It assumed a ΛCDM cosmology with parameters based on combined analysis of the 2dFGRS (Colless et al. 2001) and the first year WMAP data (Spergel et al. 2003). The parameters are: $\Omega_m = 0.25$, $\Omega_{\rm b} = 0.045$, $\Omega_\Lambda = 0.75$, $n = 1$, $\sigma_8 = 0.9$ and $H_0 = 73\ {\rm km\ s^{-1}\ Mpc^{-1}}$. These parameters differ slightly from the more recent best fit values (Larson et al. 2011) but the relatively small off-sets are not significant for most of the issues discussed in this paper, as there are much larger uncertainties in star formation and reionization parameters. There are 2160^3 particles in MS II, the box size is $100\ h^{-1}\ {\rm Mpc}$, the softening length is $1\ h^{-1}\ {\rm kpc}$, and the particle mass is $6.9{\times}10^6\ h^{-1}\ M_\odot$.

Guo et al. (2011) developed a semi-analytical model based on the MS II. This model is an extension and improvement of earlier models based on the MS (Springel et al. 2005; Croton et al. 2006; De Lucia & Blaizot 2007). In this model, central galaxies, satellite galaxies in subhalos and

orphan galaxies which had lost their subhalos are distinguished. The baryonic content of the galaxies is split into five components, including a stellar bulge, a stellar disk, a gas disk, a hot gas halo, and an ejecta reservoir. In addition, intra-cluster light is also included. The model keeps track of various processes involved in galaxy formation, including gas heating and cooling, evolution of the stellar and gas disks, star formation, supernova feedback, gas striping in groups and clusters, merger and tidal disruption, bulge formation, black hole growth and AGN feedback, metal enrichment, and photo-heating of the pregalactic gas by the UV background after reionization. A Chabrier initial mass function (IMF) (Chabrier 2003) is adopted, and this IMF has fewer low-mass stars than the Salpeter IMF. The model uses the stellar population synthesis model of Bruzual & Charlot (2003), and the dust extinction model developed in Guo & White (2009). It predicts observable properties, such as the stellar mass function, mass-size relation, distribution of galaxies within cluster and group halos, morphological type, black hole mass – bulge mass relation, low redshift galaxy luminosity function for different observing bands, stellar mass-halo mass relation, cold gas metallicity, galaxy color distribution, Tully-Fisher relation, satellite luminosity function, and autocorrelation function for different masses. Some of these predictions are compared with observations to fix the model parameters. Compared with an earlier semi-analytical model (De Lucia & Blaizot 2007), which overpredicts the abundance of galaxies with mass near or below $10^9\ M_\odot$ when applied to the MS II, this model improved the treatment of a number of physical processes, including the treatment of supernova feedback, reincorporation of ejected gas, sizes of galaxies, the treatment of satellite galaxies which are outside the R_{200} but belong to the same group, and environmental effects. The model is adjusted to best fit the observational data on galaxies at $z \sim 0$, as there are much more high quality observational data available at low redshifts, and they are subject to less selection effects. In this paper we adopt this model as our *model A* and apply it to the semi-numerical simulation of reionization.

While the predictions of this semi-analytical model are in good agreement with many observations at $z \lesssim 1$, and the abundance of luminous galaxies is also consistent with observations at $z \lesssim 3$, the predicted high redshift SFRs are systematically lower than the observed values (see fig. 22 of Guo et al. 2011 and discussions there). This is not simply a problem with this particular model, for it is well known that if the observed SFR is integrated over redshifts, the luminosity function of galaxies would be overpredicted (c.f. Wilkins et al. 2008). In fact, Guo et al. (2011) argued that even the present model might have overpredicted the abundance of low mass galaxies at high redshifts. However, as we shall see in the next section, with this model the ionizing photon production rate might be too low to allow the universe to be reionized at $z > 6$.

There have been other semi-analytical studies which tried to accommodate more of the high redshift SFR observations. For example, Raičević et al. (2011) presented a model in which major mergers can trigger starbursts, so that most of the gas in the merging galaxies collapse and form stars in a short time. In such a scenario the stars can form with a more top heavy IMF, and the number of ionizing photons would be increased dramatically. Major mergers are more frequent at high redshifts, so this model can be expected to increase the production of ionizing photons by a factor of 5 to 10 during the EoR.

To achieve a higher photon production rate during the EoR, we may consider a more top heavy IMF as Raičević et al. (2011) did. Strictly speaking, once a semi-analytical model is set, its model assumptions or parameters such as the IMF should not be altered, because the feedback would change subsequent star formation, and if one ran the full semi-analytical model with the new assumptions and compared the results with observations, a different set of parameters would be obtained. However, as we noted above, at present there is a conflict between the low redshift abundance and high redshift SFR, which cannot be easily solved. So to illustrate the effect of change, here we will just make a simple modification to the IMF, and examine its impact without considering the feedback. In our *model B*, we make an assumption similar to Raičević et al. (2011), that a major merger will trigger a starburst, and the IMF in starburst galaxies is very top heavy with an index of

0 and a mass range of $(0.15 - 120 M_{\odot})$. By doing this, more than half of the newly formed stars are massive, and the number of ionizing photons is about 10 times that in *model A*.

As *model B* may be too extreme, we also consider a *model C*. As noted above, during the EoR, many of the stars form in metal free or very low metallicity regions, which may have a top heavy IMF. Furthermore, even for the same mass, the metal-poor stars produce more ionizing photons. Here, we do not assume the flat IMF as in *model B*, but instead consider a more moderate model as suggested in Schaerer (2003), who examined the spectral properties of the ionizing continua, the Lyman break and recombination lines in starbursts and constant star formation phase, for metallicity from 0 up to solar metallicity. We adopt a Salpeter IMF for all galaxies, using a mass range of (1–500 $M_{\odot}$) with index of 2.3 for galaxies with zero metallicity, and mass range of $(1 - 100\ M_{\odot})$ with index of 2.55 for the galaxies with higher metallicity. Applying these results, the procedure in our simulation with *model C* is

(1) The ionizing luminosity for a galaxy at a given redshift is determined by its metallicity, which is determined by the metallicity of the cold gas at the last redshift;
(2) We interpolate the property of the stellar population from Schaerer (2003) and Bruzual & Charlot (2003) to obtain the luminosity;
(3) Integrate the luminosity in the past to get the number of ionizing photons;
(4) Generate the ionizing field with the number of ionizing photons from step 3 and IGM density.

We may estimate the mean metallicity of the newly formed stars from the the metallicity in the cold gas of the halo. However, in the original semi-analytical model, newly formed halos (i.e. without progenitors), regardless of redshift, will always be metal free, as the metals are not transferred out to the IGM in that model. In reality, the IGM will be polluted by galactic winds, which blow the enriched gas out of the halo, and Lyman alpha forest observations show that the IGM has already been contaminated at $z > 3$ (Schaye et al. 2003). Thus, even the newly formed halos should contain some amount of metals. As a remedy to this, we set the metallicity in the cold gas of the newly formed halos to be the average value of the whole simulation box, which is calculated by the metal production in the original semi-analytical model. In Figure 1, we plot the SFR of different metallicities according to this model, where the Pop I, II and III stars are represented by the dotted, dashed and dot-dashed curves, respectively, and the black solid curve represents the total SFR. While initially (at very high redshift) the Pop III had the largest SFR, this was soon surpassed by Pop II ($z \sim 16$), which was in turn surpassed by Pop I at a fairly high redshift ($z \sim 12$). The formation of Pop III stars declined at $z \sim 10$, and fluctuated a little at low redshift but stayed at a low value. In this model we have assumed that the metals are uniformly distributed; the non-uniform distribution of metals may allow a higher production rate of metal-free or metal-poor stars.

In Figure 2, we plot the evolution of the cumulative production rate of ionizing photons due to stars of different metallicities in our *model C*. We see that during most of the EoR, the contribution from the Pop II stars dominates. The Pop III stars could make up major contributions only at fairly high redshifts, but level off at $z \sim 10$ in this model. The Pop I stars have a higher SFR, but do not make up the major contribution to the ionizing photons.

4 RESULTS

Let us first take a look at the global production rate of ionizing photons in our model. In Figure 3, we plot the ratio between the number of ionizing photons from stars and the number of hydrogen atoms per comoving volume; here the escape fraction and recombination number are not included. Thus, if we assume $f_{\rm esc} \sim 0.15$ and $N_{\rm rec} \sim 3$, the ionizing photon-to-baryon ratio has to be greater than 20 for the universe to be reionized. The dashed line shows the result from assuming that each hydrogen atom in the stars produces on average of 3200 photons during the life time of the star, which corresponds to the normal stellar population given by our *model A*. The dot-dashed line shows the

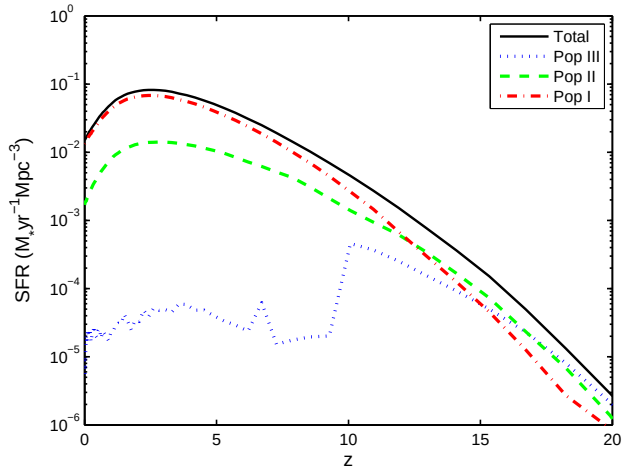

Fig. 1 The SFR of different metallicities in our *model C*.

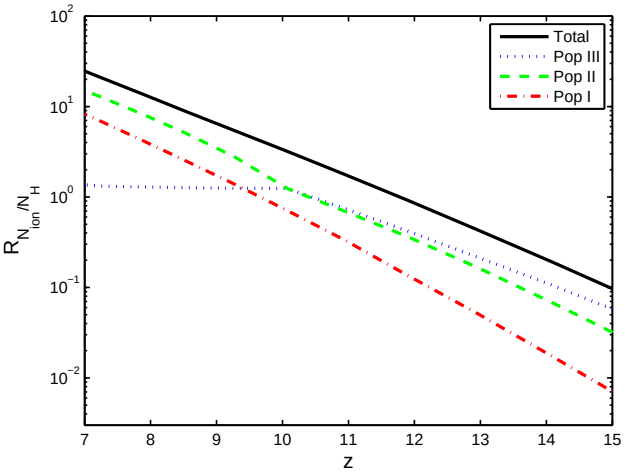

Fig. 2 The number of ionizing photons of different metallicities in our *model C*.

result for our *model B*, which produced many more photons, as we assumed a very top heavy IMF for starburst galaxies. The black solid line corresponds to our *model C*, which assumed a mixture of Pop I, Pop II and Pop III stars. From the figure, we can see that for *model A*, it is very difficult to ionize the universe by $z \sim 6$, even if large escape fractions and low recombination rates are assumed. *Model B* could ionize the universe at relatively early time, perhaps $z \sim 8$. In *model C*, reionization occurred at $z \sim 7$, which is still much later than the $z_{\rm re} = 9$ given by the WMAP data (Larson et al. 2011).

We may also compare the galaxy UV luminosity function with observations at high redshifts. Figures 4–5 show the 1500 Å luminosity functions predicted by our *model A* and *model C* at $z = 7.88$ and $z = 7.27$ respectively, and for comparison we also plot the measured luminosity function at 1600 Å from Bouwens et al. (2011). We see that our *model A* is in excellent agreement with the luminosity function, even though its prediction on SFR falls below many observations. Our *model C*

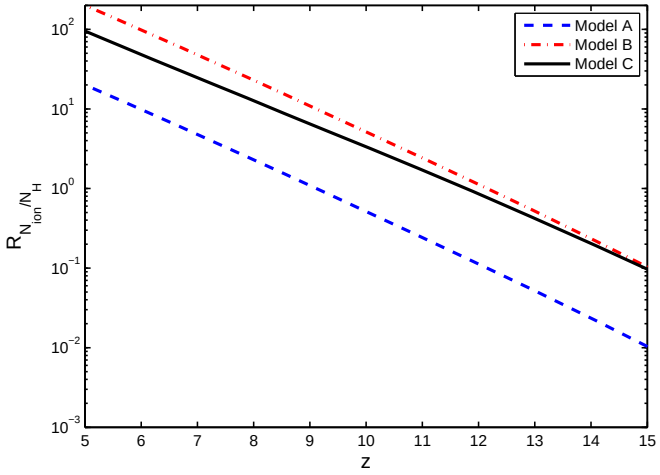

Fig. 3 The ratio between number of ionizing photons from stars and number of hydrogen atoms for the three models we considered.

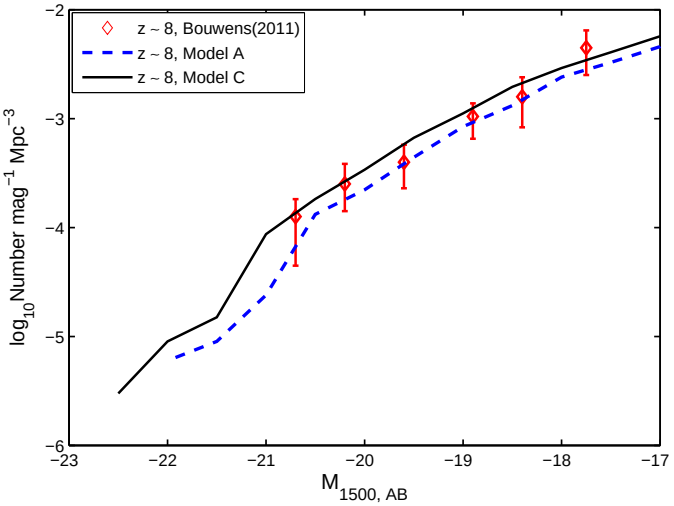

Fig. 4 The luminosity function at $z = 7.88$. The data points are from Bouwens et al. (2011). The predictions of our *model A* and *model C* are shown as a dashed line and black solid line respectively.

overpredicts the luminosity function slightly, but given the large uncertainties in the data at present, the deviation is still acceptable.

With the semi-analytical model of ionizing photon production in place, we can now use the procedure described in Section 2 to simulate the reionization process. Figure 6 shows the reionization process of our simulation box for our *model C*. The black colored regions are neutral, while the white ones are ionized. The redshifts are, from upper left to lower right, 14.9, 11.9, 10.9, 9.3, 7.88 and 7.27.

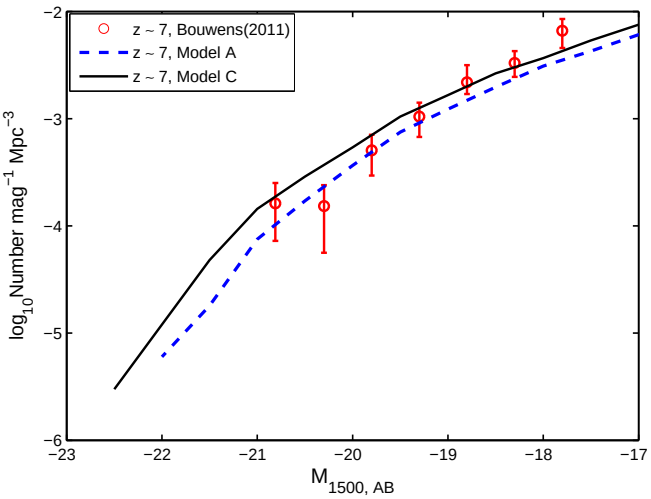

Fig. 5 The same as Fig. 4, but for $z = 7.27$.

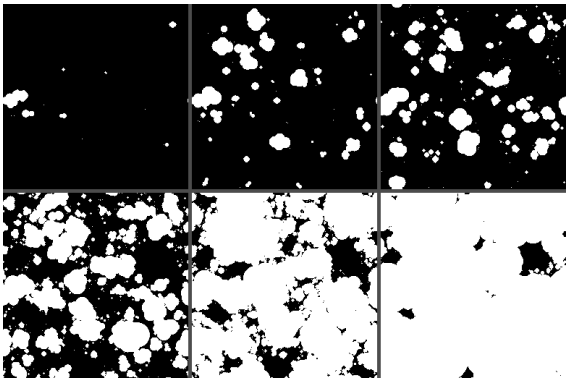

Fig. 6 Ionizing map of our *model C*, with parameters $f_{\rm esc} = 0.15$ and $N_{\rm rec} = 3$. From the upper left to the lower right, the redshifts are 14.9, 11.9, 10.9, 9.3, 7.88 and 7.27. Black and white regions correspond to HI and HII regions, and the pixels represent cases of being neutral or ionized.

We can see that the universe is mostly neutral before redshift 12, but with some bubbles representing HII regions. Around redshift 9, the bubbles begin to overlap, and by $z = 7$, most of the universe is ionized.

How does this semi-numerical model compare with a model without the semi-analytical modeling? This depends somewhat on the particular model we use as well as the redshift. However, in some cases the difference can be quite obvious.

In Figure 7 we plot the ionization at redshift $z = 6.7$ for our *model A*. Here, we have chosen to show *model A* for comparison because *model A* uses the original semi-analytical model. As we can see from the figure, while the large scale distributions of the HI and HII regions are similar, we see that in the model without semi-analytical modeling, there are more small HII regions which are absent in the model with it. In the model without semi-analytical galaxy formation, the number of

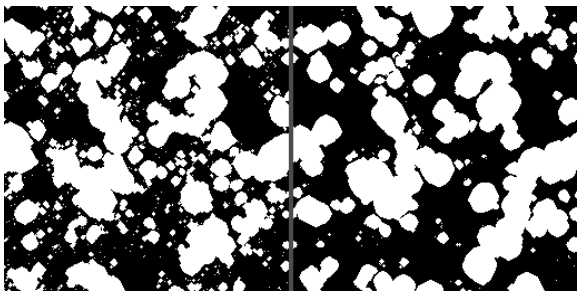

Fig. 7 Comparison of ionization map produced by the semi-numerical simulation without (*left*) and with (*right*) semi-analytical models.

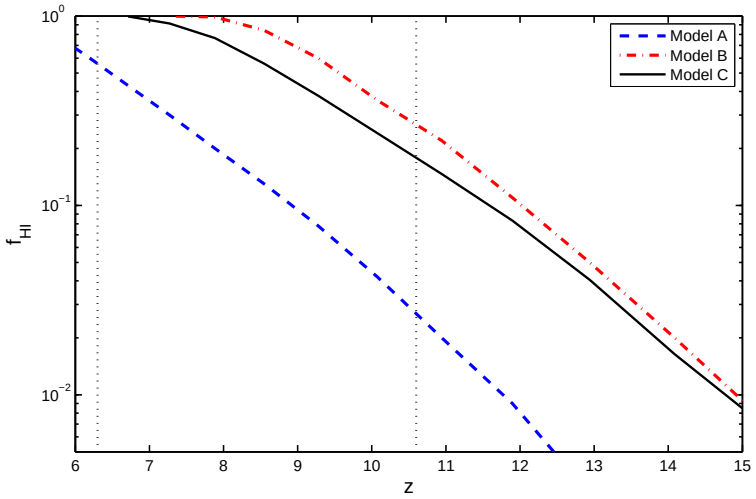

Fig. 8 Evolution of the ionization fraction for the different models. Here we take $f_{\rm esc} = 0.15$ and $N_{\rm rec} = 3$. The vertical lines mark the reionization redshifts constrained by the Gunn-Peterson trough of quasars and WMAP observations.

photons are predicted from the dark matter halos, and as a result, some halos which do not contain stars were also assumed to produce ionizing photons. This would not affect large HII regions, but in the neutral regions, small HII regions are produced around these small halos. This can significantly affect the topology of the ionization map, giving it a more poriferous appearance. In the model with semi-analytical modeling, on the other hand, only galaxies contribute to ionizing photons, while the starless minihalos do not contribute, so the HI and HII regions are more well separated with a monolithic appearance.

In Figure 8 we plot the evolution of the global ionization fraction for the different models, where we assumed $f_{\rm esc} = 0.15$ and $N_{\rm rec} = 3$. These results are consistent with the ratio between the ionizing number and hydrogen number in Figure 3. For *model A*, the reionization happened very

late. Even at $z = 6$, the universe is still not ionized in this model. In *model B*, the ionization occurred at $z \sim 8$. In *model C*, the universe is fully ionized at $z \sim 7$, and it reached $f_{\rm HII} = 0.5$ at $z \sim 9$.

5 SUMMARY AND DISCUSSION

In this paper we incorporated a MS II based semi-analytical model of galaxy formation (Guo et al. 2011) in the semi-numerical simulation of reionization, which was shown to be a good approximation to the radiative transfer computation, but with much less computational cost. SFR is given by the semi-analytical model and is then used to compute the production rate of ionizing photons in each galaxy. As this semi-analytical model is exclusively designed to best fit the observations at $z \sim 0$, there are some discrepancies between its predictions and high redshift observations. This model, denoted by our *model A*, predicts an SFR lower than the observed values at high redshifts, but it does reproduce the observed UV luminosity function at $z \sim 7 - 8$, thus clearly revealing the conflict between the observed luminosity function and SFR at high redshifts. However, the ionizing photon production rate for this model is too low, such that the universe cannot be reionized at $z > 6$ for an escape fraction of $f_{\rm esc} = 0.15$ and the mean number of recombinations $N_{\rm rec} = 3$.

To remedy this problem, we also considered two simple revised models. These models assumed the same SFR as the original model, but adopted a different IMF for star formation. In *model B*, a flat IMF is assumed. This model can produce about 10 times the ionizing photons of *model A*, and the universe is reionized at $z = 8$. In *model C*, we assumed a top heavy IMF but with similar slopes, and we also considered the production rate of ionizing photons to be a function of metallicity of the newly formed stars. The metallicity of the star is determined by the metallicity of the cold gas in the halo, which was given in the original semi-analytical model. We also assumed a metallicity floor in the IGM as given by the average metallicity of the simulation box. This model predicts that Pop II stars are the major sources of ionizing photons during the EoR, even though the Pop I SFR is higher. The predicted UV luminosity function at $z \sim 7 - 8$ of *model C* is only slightly higher than the observed value. The universe is ionized at $z \sim 7$ in this model.

Armed with the semi-analytical model, we simulate reionization history with the semi-numerical method. The addition of the semi-analytical model could significantly affect the topology of the neutral and ionized regions. While it is somewhat dependent on the particular model and redshift, in some cases the difference is quite large. Without the semi-analytical model of galaxy formation, we may incorrectly assume ionizing photons were produced by starless minihalos in HI regions, and this may produce a more poriferous appearance. With the semi-analytical model, the ionizing photons only come from galaxies, not from all minihalos, so the HII regions appeared to be more monolithic and well separated from HI regions.

We have made some simplifications in this research. For example, we have adopted a simple constant mean value for the escape fraction and number of recombinations. In reality, both of these may evolve with redshift, or even vary with different galaxies. We have assumed a simple two phase model of IGM such that at any given point it is either fully neutral or fully ionized, so that partial ionization is not considered, and we do not consider the effect of quasar formation. However, within the plausible range of the parameters, these effects are unlikely to change our result qualitatively. As the aim of this paper is to illustrate the use of a semi-analytical model of galaxy formation in semi-numerical modeling, we do not try to model these complications.

There are certain limitations in our present work. Perhaps the most important one is that our models B and C are not completely self-consistent. We have assumed that they have the same SFR evolution as given by *model A*, but with a modified IMF and ionizing photon production. However, once the IMF of the model is changed, the star formation history would not be the same, because the feedback effect would be different, and that would change the subsequent accretion and star formation. If we hope to have a similar star formation history with this modified IMF, we must assume a lower strength of feedback. Furthermore, the reionization itself may also affect the galaxy

formation process. To be really self-consistent, one has to modify the semi-analytical model itself. This will be the next step in our research.

As we discussed above, the semi-numerical simulation combined with the semi-analytical galaxy formation model provides a good approximation of reionization history. It allows us to investigate large parameter ranges in a short time, and more importantly, connects the observations of galaxies to the reionizations. This approach could help us better understand the galaxy formation process.

Acknowledgements We thank Youjun Lu for helpful discussions. This work is supported by the MOST 863 Project (No. 2012AA121701), the National Natural Science Foundation of China (Grant No. 11073024), CAS grant KJCX2-EW-W01 and the John Templeton Foundation.

References

Ahn, K., Iliev, I. T., Shapiro, P. R., et al. 2012, ApJ, 756, L16
Altay, G., Croft, R. A. C., & Pelupessy, I. 2008, MNRAS, 386, 1931
Aubert, D., & Teyssier, R. 2008, MNRAS, 387, 295
Barkana, R., & Loeb, A. 2001, Phys. Rep., 349, 125
Becker, R. H., Fan, X., White, R. L., et al. 2001, AJ, 122, 2850
Bouwens, R. J., Illingworth, G. D., Oesch, P. A., et al. 2011, ApJ, 737, 90
Bouwens, R. J., Illingworth, G. D., Oesch, P. A., et al. 2012, ApJ, 752, L5
Bower, R. G., Benson, A. J., Malbon, R., et al. 2006, MNRAS, 370, 645
Bowman, J. D., & Rogers, A. E. E. 2010, Nature, 468, 796
Boylan-Kolchin, M., Springel, V., White, S. D. M., Jenkins, A., & Lemson, G. 2009, MNRAS, 398, 1150
Bradley, L. D., Trenti, M., Oesch, P. A., et al. 2012, arXiv: 1204.3641
Bruzual, G., & Charlot, S. 2003, MNRAS, 344, 1000
Bunker, A. J., Wilkins, S., Ellis, R. S., et al. 2010, MNRAS, 409, 855
Chabrier, G. 2003, PASP, 115, 763
Ciardi, B., Ferrara, A., & White, S. D. M. 2003, MNRAS, 344, L7
Cole, S., Aragon-Salamanca, A., Frenk, C. S., Navarro, J. F., & Zepf, S. E. 1994, MNRAS, 271, 781
Cole, S., Lacey, C. G., Baugh, C. M., & Frenk, C. S. 2000, MNRAS, 319, 168
Colless, M., Dalton, G., Maddox, S., et al. 2001, MNRAS, 328, 1039
Croton, D. J., Springel, V., White, S. D. M., et al. 2006, MNRAS, 365, 11
De Lucia, G., & Blaizot, J. 2007, MNRAS, 375, 2
Fan, X., Narayanan, V. K., Strauss, M. A., et al. 2002, AJ, 123, 1247
Finlator, K., Özel, F., & Davé, R. 2009, MNRAS, 393, 1090
Furlanetto, S. R., Lidz, A., Loeb, A., et al. 2009, in astro2010: The Astronomy and Astrophysics Decadal Survey, 2010, 82 (arXiv: 0902.3259)
Furlanetto, S. R., Zaldarriaga, M., & Hernquist, L. 2004a, ApJ, 613, 16
Furlanetto, S. R., Zaldarriaga, M., & Hernquist, L. 2004b, ApJ, 613, 1
Gnedin, N. Y. 2000, ApJ, 542, 535
Grazian, A., Castellano, M., Koekemoer, A. M., et al. 2011, A&A, 532, A33
Guo, Q., White, S., Boylan-Kolchin, M., et al. 2011, MNRAS, 413, 101
Guo, Q., & White, S. D. M. 2009, MNRAS, 396, 39
Harker, G., Zaroubi, S., Bernardi, G., et al. 2010, MNRAS, 405, 2492
Hatton, S., Devriendt, J. E. G., Ninin, S., et al. 2003, MNRAS, 343, 75
Ishida, E. E. O., de Souza, R. S., & Ferrara, A. 2011, MNRAS, 418, 500
Iwata, I., Inoue, A. K., Matsuda, Y., et al. 2009, ApJ, 692, 1287
Joudaki, S., Doré, O., Ferramacho, L., Kaplinghat, M., & Santos, M. G. 2011, Physical Review Letters, 107, 131304

Kauffmann, G., Colberg, J. M., Diaferio, A., & White, S. D. M. 1999, MNRAS, 303, 188
Kauffmann, G., White, S. D. M., & Guiderdoni, B. 1993, MNRAS, 264, 201
Larson, D., Dunkley, J., Hinshaw, G., et al. 2011, ApJS, 192, 16
Lorenzoni, S., Bunker, A. J., Wilkins, S. M., et al. 2011, MNRAS, 414, 1455
Madau, P., Meiksin, A., & Rees, M. J. 1997, ApJ, 475, 429
Maselli, A., Ferrara, A., & Ciardi, B. 2003, MNRAS, 345, 379
McQuinn, M., Lidz, A., Zahn, O., et al. 2007, MNRAS, 377, 1043
Mellema, G., Iliev, I. T., Alvarez, M. A., & Shapiro, P. R. 2006, New Astron., 11, 374
Mesinger, A., & Furlanetto, S. 2007, ApJ, 669, 663
Mesinger, A., Furlanetto, S., & Cen, R. 2011, MNRAS, 411, 955
Mitra, S., Choudhury, T. R., & Ferrara, A. 2011, MNRAS, 413, 1569
Ota, K., Iye, M., Kashikawa, N., et al. 2010, ApJ, 722, 803
Paciga, G., Chang, T.-C., Gupta, Y., et al. 2011, MNRAS, 413, 1174
Parsons, A. R., Backer, D. C., Foster, G. S., et al. 2010, AJ, 139, 1468
Pen, U.-L., Chang, T.-C., Hirata, C. M., et al. 2009, MNRAS, 399, 181
Petkova, M., & Springel, V. 2009, MNRAS, 396, 1383
Raičević, M., Theuns, T., & Lacey, C. 2011, MNRAS, 410, 775
Rauch, M., Miralda-Escude, J., Sargent, W. L. W., et al. 1997, ApJ, 489, 7
Razoumov, A. O., Norman, M. L., Abel, T., & Scott, D. 2002, ApJ, 572, 695
Salvaterra, R. 2012, Memorie della Societa Astronomica Italiana Supplementi, 21, 54
Santos, M. G., Silva, M. B., Pritchard, J. R., Cen, R., & Cooray, A. 2011, A&A, 527, A93
Schaerer, D. 2003, A&A, 397, 527
Schaye, J., Aguirre, A., Kim, T.-S., et al. 2003, ApJ, 596, 768
Shapley, A. E., Steidel, C. C., Pettini, M., Adelberger, K. L., & Erb, D. K. 2006, ApJ, 651, 688
Siana, B., Teplitz, H. I., Colbert, J., et al. 2007, ApJ, 668, 62
Sokasian, A., Abel, T., & Hernquist, L. E. 2001, New Astron., 6, 359
Somerville, R. S., & Primack, J. R. 1999, MNRAS, 310, 1087
Spergel, D. N., Verde, L., Peiris, H. V., et al. 2003, ApJS, 148, 175
Springel, V., White, S. D. M., Jenkins, A., et al. 2005, Nature, 435, 629
Springel, V., White, S. D. M., Tormen, G., & Kauffmann, G. 2001, MNRAS, 328, 726
Trac, H., & Cen, R. 2007, ApJ, 671, 1
Weinmann, S. M., Kauffmann, G., von der Linden, A., & De Lucia, G. 2010, MNRAS, 406, 2249
White, S. D. M., & Frenk, C. S. 1991, ApJ, 379, 52
Wilkins, S. M., Bunker, A. J., Ellis, R. S., et al. 2010, MNRAS, 403, 938
Wilkins, S. M., Trentham, N., & Hopkins, A. M. 2008, MNRAS, 385, 687
Yan, H., Finkelstein, S. L., Huang, K.-H., et al. 2011a, arXiv: 1112.6406
Yan, H., Yan, L., Zamojski, M. A., et al. 2011b, ApJ, 728, L22
Yue, B., & Chen, X. 2012, ApJ, 747, 127
Zahn, O., Lidz, A., McQuinn, M., et al. 2007, ApJ, 654, 12
Zahn, O., Mesinger, A., McQuinn, M., et al. 2011, MNRAS, 414, 727
Zaldarriaga, M., Furlanetto, S. R., & Hernquist, L. 2004, ApJ, 608, 622